THE JOURNAL OF BIOLOGICAL CHEMISTRY
Vol. 278, No. 32, Issue of August 8, pp. 29496–29501, 2003
Printed in U.S.A.

Inhibition of Calcium Uptake via the Sarco/Endoplasmic Reticulum Ca^{2+}-ATPase in a Mouse Model of Sandhoff Disease and Prevention by Treatment with *N*-Butyldeoxynojirimycin*

Received for publication, March 24, 2003, and in revised form, May 15, 2003
Published, JBC Papers in Press, May 19, 2003, DOI 10.1074/jbc.M302964200

Dori Pelled‡§, Emyr Lloyd-Evans‡§¶, Christian Riebeling‡‖, Mylvaganam Jeyakumar¶, Frances M. Platt¶‡‡, and Anthony H. Futerman‡§§**

From the ‡Department of Biological Chemistry, Weizmann Institute of Science, Rehovot 76100, Israel and ¶Department of Biochemistry, Glycobiology Institute, University of Oxford, South Parks Road, Oxford OX1 3QU, United Kingdom

Gangliosides are found at high levels in neuronal tissues where they play a variety of important functions. In the gangliosidoses, gangliosides accumulate because of defective activity of the lysosomal proteins responsible for their degradation, usually resulting in a rapidly progressive neurodegenerative disease. However, the molecular mechanism(s) leading from ganglioside accumulation to neurodegeneration is not known. We now examine the effect of ganglioside GM2 accumulation in a mouse model of Sandhoff disease (one of the GM2 gangliosidoses), the Hexb−/− mouse. Microsomes from Hexb−/− mouse brain showed a significant reduction in the rate of Ca^{2+}-uptake via the sarco/endoplasmic reticulum Ca^{2+}-ATPase (SERCA), which was prevented by feeding Hexb−/− mice with *N*-butyldeoxynojirimycin (NB-DNJ), an inhibitor of glycolipid synthesis that reduces GM2 storage. Changes in SERCA activity were not due to transcriptional regulation but rather because of a decrease in V_{max}. Moreover, exogenously added GM2 had a similar effect on SERCA activity. The functional significance of these findings was established by the enhanced sensitivity of neurons cultured from embryonic Hexb−/− mice to cell death induced by thapsigargin, a specific SERCA inhibitor, and by the enhanced sensitivity of Hexb−/− microsomes to calcium-induced calcium release. This study suggests a mechanistic link among GM2 accumulation, reduced SERCA activity, and neuronal cell death, which may be of significance for delineating the neuropathophysiology of Sandhoff disease.

The GM2 gangliosidoses are a group of inherited metabolic disorders caused by mutations in any of three genes, the *HEXA* gene, resulting in Tay-Sachs disease, the *HEXB* gene, resulting in Sandhoff disease, and the *GM2A* gene, resulting in GM2 activator deficiency (1, 2). The *HEXA* and *HEXB* genes code for the β-hexosaminidase α- and β-subunits, respectively, which dimerize to produce two forms of the enzyme, A (αβ) and B (ββ), and a minor form, S (αα). In both Tay-Sachs and Sandhoff disease (α- and β-subunit deficiency, respectively), there is a deficit of hexosaminidase A (αβ) and, as a consequence, massive accumulation of ganglioside GM2 in the brain (3). As in all lysosomal storage diseases, significant clinical heterogeneity is observed, varying from infantile-onset, rapidly progressive neurological disease culminating in death before 4 years of age to late-onset, sub-acute or chronic progressive neurological disease (4).

Few molecular details are available that delineate the pathway leading from GM2 accumulation to neurological disease. In the current study, we analyze the effect of GM2 accumulation in neuronal tissues obtained from mice homozygous for the disrupted *HEXB* gene (5, 6), a model of Sandhoff disease. The Hexb−/− mouse shows increased neuronal GM2 storage in most brain areas (5), neuronal apoptosis (6), changes in rates of axonal and dendritic growth (7), and severe neurological disturbances causing death by ~4 months of age. We demonstrate that brain microsomes and neurons cultured from these mice show dramatically reduced levels of Ca^{2+}-uptake via the sarco/endoplasmic reticulum Ca^{2+}-ATPase (SERCA),[1] which is not related to transcriptional regulation of SERCA but rather to changes in V_{max}. Impairment of SERCA activity usually results in neuronal cell dysfunction and/or death (8, 9), and our observations that Ca^{2+}-uptake via SERCA is severely impaired upon GM2 accumulation may suggest a molecular mechanism to explain, at least in part, the neuropathophysiology in Sandhoff disease. This is supported by our observation that SERCA activity is essentially normal in 3-month-old Hexb−/− mice fed with the glycolipid synthesis inhibitor *N*-butyldeoxynojirimycin (NB-DNJ) (10, 11), which correlates with the delayed symptom onset and increased life expectancy of these mice (12).

EXPERIMENTAL PROCEDURES

Materials—Gangliosides GM3, GM2, and GM1 were obtained from Matreya (Pleasant Gap, PA). Antipyrylazo III, thapsigargin, creatine phosphokinase, phosphocreatine, and ATP were from Sigma. $^{45}Ca^{2+}$ (30 mCi/mg) was from Amersham Biosciences. NB-DNJ was from Searle Monsanto and Oxford GlycoSciences. The anti-SERCA2 antibody (N-19) was from Santa Cruz Biotechnology (Santa Cruz, CA), and a horseradish peroxidase-conjugated rabbit anti-goat secondary antibody was from Jackson Laboratories (West Grove, PA). Silica gel 60 thin layer chromatography plates were from Merck. All solvents were of analytical grade and were purchased from Biolab (Jerusalem, Israel). Oligonucleotides were synthesized by the Weizmann Institute Oligonucleotide and Peptide Synthesis Facility.

* Hexb mice were obtained from the laboratory of Prof. Dr. Konrad Sandhoff and Dr. Gerhild van Echten-Deckert, University of Bonn, in the framework of a grant from the German-Israel Foundation for Scientific Research. The costs of publication of this article were defrayed in part by the payment of page charges. This article must therefore be hereby marked "*advertisement*" in accordance with 18 U.S.C. Section 1734 solely to indicate this fact.

§ Contributed equally to this work.

‖ Supported by a Research Training Network Fellowship HPRN-CT-2000-00077 from the European Union.

** Supported by The Wellcome Trust.

‡‡ Lister Institute Research Fellow.

§§ To whom correspondence should be addressed. Tel.: 972-8-9342704; Fax: 972-8-9344112; E-mail: tony.futerman@weizmann.ac.il.

[1] The abbreviations used are: SERCA, sarco/endoplasmic reticulum Ca^{2+}-ATPase; CICR, calcium-induced calcium-release; ER, endoplasmic reticulum; NB-DNJ, *N*-butyldeoxynojirimycin; RT, reverse transcription; MOPS, 4-morpholinepropanesulfonic acid.

Hexb Colony—A mouse model of Sandhoff disease (the Hexb−/− mouse) (5–7) was maintained in the Experimental Animal Center of the Weizmann Institute of Science (7). Wild type (Hexb+/+) mice were bred with each other, as were Hexb−/− mice, to obtain homozygous offspring. The genotype of the mice was determined by PCR using genomic DNA extracted from mouse tails (13). A similar Hexb colony, maintained in the Glycobiology Institute at the University of Oxford, Oxford, United Kingdom, was used for the studies in which Hexb−/− mice were fed with NB-DNJ. Mice were treated from weaning at 3 weeks with 1200 mg/kg/day of NB-DNJ.

Lipid Analysis—GM2 levels were determined in Hexb−/− mouse brains at various ages after birth and compared with Hexb+/+ mice (11). GM2 levels were determined in microsomes after glycosphingolipid extraction (14, 15), separation by thin layer chromatography using chloroform:methanol:9.8 mM $CaCl_2$ (60:35:8, vol:vol:vol) as the developing solvent, and resorcinol staining. Ganglioside GM2 was identified using an authentic standard.

Hexb Brain Microsomes—Hexb mice were sacrificed after 3–4 months, and their brains were removed, separated into cerebral cortex and cerebellum, rapidly frozen in liquid N_2, and stored at −80 °C; in one set of experiments, microsomes were prepared from embryonic day 17 (E17) mouse cortices. Cortical microsomes (from 12–25 mice) were prepared essentially as described (16) with some modifications. Tissue was suspended at a ratio of 1:4 (w/v) in ice-cold Buffer A (0.32 M sucrose, 20 mM HEPES-KOH, pH 7.0, containing 0.4 mM phenylmethylsulfonyl fluoride, leupeptin (0.8 μg/ml), and aprotinin (1.4 trypsin inhibitory units)), and homogenized at 4 °C using eight up and down strokes of a rotating Potter-Elvehjem homogenizer. After centrifugation ($700 \times g_{av}$, 10 min), the resulting pellet (P1) was gently resuspended in ¼ of the original volume of Buffer A and centrifuged ($700 \times g_{av}$, 10 min), and the two supernatants were pooled (S1). Mitochondria were removed by centrifugation ($8{,}000 \times g_{av}$, 45 min) of S1, and the resulting supernatant (S2) was centrifuged ($115{,}000 \times g_{av}$, 90 min) to obtain a microsomal pellet (P3), which was resuspended in 0.4–0.8 ml of Buffer A. Protein was determined (17), and the microsomes were subsequently flash-frozen in liquid N_2. Microsomes were stored at −80 °C and used for up to several weeks after their preparation, during which time there was no change in their activity with respect to Ca^{2+}-release and -uptake.

Spectrophotometric Assay of Ca^{2+}-Uptake—Ca^{2+}-Uptake was measured by a spectrophotometric assay using the Ca^{2+}-sensitive dye, antipyrylazo III (16, 18, 20), with some modifications. Mouse brain microsomes (330 μg in 8–15 μl of Buffer A) were added to 0.95 ml of 8 mM NaMOPS, pH 7.0, 40 mM KCl, 62.5 mM K_2HPO_4, and 250 μM antipyrylazo III in a plastic cuvette containing a magnetic stir bar, to which 1 mM MgATP, 40 μg/ml creatine phosphokinase, and 5 mM phosphocreatine, pH 7.0, were added. Ca^{2+}-Uptake and -release were measured in a Cary spectrophotometer (Varian Australia Pty Ltd.) at 37 °C by subtracting A_{790} from A_{710} at 2-s intervals. The effect of exogenously added GM3, GM2, and GM1, dissolved in absolute ethanol, was tested by their addition 5 min before Ca^{2+}-loading. The rate of Ca^{2+}-uptake into microsomes was calculated by measuring the linear portion of the slope after addition of Ca^{2+}.

Kinetic Assay of SERCA—Ca^{2+}-Uptake by SERCA was determined radiometrically using a rapid filtration technique (21). Mouse cortical microsomes (350 μg protein) were incubated at 37 °C in 1.5 ml of Buffer B (40 mM imidazole, pH 7.0, 100 mM KCl, 5 mM $MgCl_2$, 5 mM NaN_3, 5 mM potassium oxalate, 0.5 mM EGTA, 1 μM ruthenium red (21) (which blocks spontaneous Ca^{2+}-release via the ryanodine receptor (22)), 10 μCi $^{45}Ca^{2+}$, and $CaCl_2$, to yield the required final concentration of free Ca^{2+} (determined using an algorithm (23) and software available at www.stanford.edu/~cpatton/maxc.html). Ca^{2+}-Uptake was initiated by addition of ATP and terminated after 1, 3, and 5 s by addition of 3 ml of ice-cold washing solution (20 mM HEPES, pH 7.4, 150 mM KCl, 1.4 mM $MgCl_2$, and 2 mM KH_2PO_4) (24), followed by filtration through a HAWP 0.45-μm Millipore filter in a Millipore filtration device. The initial rate of Ca^{2+}-uptake (v_o) was calculated by linear regression analysis. The kinetic coefficients of Ca^{2+}-uptake were calculated according to Equation 1 (25), using non-linear regression analysis (Origin 5.0; MicroCal Software, Inc.).

$$\nu = V_{max}\frac{K_{Ca}^n}{[Ca_i]^n + K_{Ca}^n} \qquad \text{(Eq. 1)}$$

In Equation 1, V_{max} is maximum velocity, K_{Ca} is the concentration required for half-maximal activation, and n is the equivalent of the Hill coefficient. The K_{ATP} was obtained by Michaelis-Menten analysis.

RT-PCR—Total cellular RNA was prepared from individual cortices using the TRI reagent (MRC, Cincinnati, OH) or from $\sim 0.5 \times 10^6$ neurons (see below) grown on 24-mm coverslips using the RNeasy Mini Kit (Qiagen) according to the manufacturer's instructions. The RT-PCR was performed as described (26) using the Qiagen OneStep RT-PCR kit. Primers (SERCA2a: 5′-ACTTCTTGATCCTCTACGTG and 5′-AAATGGTTTAGGAAGCGGTT, 33 cycles, annealing temperature 53 °C; SERCA2b: 5′-ACTTCTTGATCCTCTACGTG (same as SERCA2a) and 5′-AGACCAGAACATATCGCTAA, 25 cycles, annealing temperature 53 °C; glyceraldehyde-3-phosphate dehydrogenase: 5′-TTAGCACCCCTGGCCAAGG and 5′-CTTACTCCTTGGAGGCCATG, 23 cycles, annealing temperature 50 °C) were designed using the MacMolly Tetra program (Softgene, Berlin, Germany), and conditions were adjusted to be within the linear phase of PCR. For sequencing, bands were excised from gels and purified using the QIAquick gel extraction kit (Qiagen) and subsequently sequenced by the DNA sequencing unit of the Weizmann Institute of Science using the respective primers.

SDS-PAGE and Western blotting—SDS-PAGE and Western blotting were performed as described (27) using a 6% separating gel. After transfer to nitrocellulose membranes, the blot was incubated with blocking buffer (Tris-buffered saline containing 3% (w/v) non-fat dried milk, 1% (w/v) bovine serum albumin, and 0.1% Tween 20) for 20 min and then incubated with an anti-SERCA2 antibody at a dilution of 1/100 in blocking buffer for 2 h. Bound antibodies were detected after washing using 25 ng/ml horseradish peroxidase-conjugated rabbit anti-goat secondary antibodies in blocking buffer for 1 h and the SuperSignal chemiluminescent detection reagent (Pierce).

Neuronal Ca^{2+}-Uptake—Embryos (embryonic day 17) were isolated, the hippocampi were removed, and hippocampal pyramidal neurons were cultured as described (7). The dissected hippocampi were dissociated by trypsinization (0.25% w/v, for 15 min at 37 °C), and the tissue was washed in Mg^{2+}/Ca^{2+}-free Hanks' balanced salt solution and dissociated by repeated passage through a constricted Pasteur pipette. Neurons were maintained in Neurobasal serum-free medium containing B27 supplements and L-glutamine (28) (Invitrogen).

For analysis of Ca^{2+}-uptake (29), neurons were plated at a density of 1.1×10^6 cells per 60-mm culture dish that contained three 24-mm polylysine-coated coverslips. Coverslips were washed in Ca^{2+}-free medium (minimal essential medium containing 50 mM HEPES, pH 7.3, 4 mM $NaHCO_3$, 11 mg/ml pyruvic acid, 1 mM glutamine, and 0.6% (w/v) glucose (30)) and transferred to a new dish containing the same medium. After 25 min at 37 °C, neurons were incubated with the calcium ionophore A23187 (1 μM) (31) for 5 min, prior to addition of 1 μCi of $^{45}Ca^{2+}$ for 30 s at 37 °C (32). The reaction was terminated by removing coverslips from the wells and washed by dipping five times in Ca^{2+}-free medium and then placing in 0.65 ml of NaOH (0.5 M) for 3 h. $^{45}Ca^{2+}$ was further extracted by adding NaOH for 16 h and then for another 2 h. NaOH extracts were pooled, and $^{45}Ca^{2+}$ was determined by liquid scintillation counting.

Neuronal Cell Death—Neurons were plated at a density of 25,000 cells per 13-mm coverslip in a 24-multiwell dish. Live and dead cells were distinguished using 2 μM calcein acetoxymethyl ester and 4 μM ethidium homodimer-1, respectively, as described in a Live/Dead® viability/cytotoxicity kit (Molecular Probes Inc.). At least 700–800 cells were counted per coverslip. Neurons were examined using a Plan 25×/0.45 numerical aperture objective of a Zeiss Axiovert 35 microscope.

RESULTS

Previous studies have shown that GM2 accumulates in adult Hexb−/− mouse brains (5). We now examine GM2 accumulation throughout brain development. Even at the earliest age measured, embryonic day 10, small but significant levels of GM2 were detected (7.6 ± 0.4 μg/10 mg dry weight), which increased to levels of 140 ± 7 μg/10 mg dry weight in 3-month-old mice (Fig. 1*A*), whereas no GM2 could be detected at any stage in Hexb+/+ brains. Significant amounts of GM2 were also detected in microsomes prepared from 3–4-month-old Hexb−/− mice, but essentially no GM2 was detected in microsomes from Hexb+/+ mice (Fig. 1*B*). A significant decrease in GM2 accumulation (Fig. 1*B*) was observed in microsomes from 120-day-old Hexb−/− mice that had been fed with NB-DNJ, similar to that reported previously for whole brain (12).

We proposed recently that changes in Ca^{2+}-homeostasis, and specifically changes in Ca^{2+}-release from intracellular stores via the ryanodine receptor (29, 33), may be responsible, at least

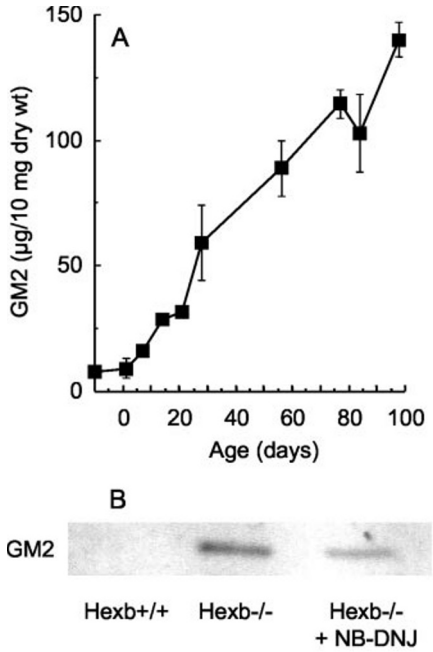

FIG. 1. **GM2 accumulation in Hexb brains and microsomes.** *A*, gangliosides were extracted from individual Hexb−/− mouse brains at the indicated ages, and GM2 was quantified. *B*, gangliosides were extracted from cortical microsomes obtained from 120-day-old Hexb+/+ and Hexb−/− mice, or from Hexb−/− mice that were fed NB-DNJ, and ganglioside GM2 was visualized by resorcinol.

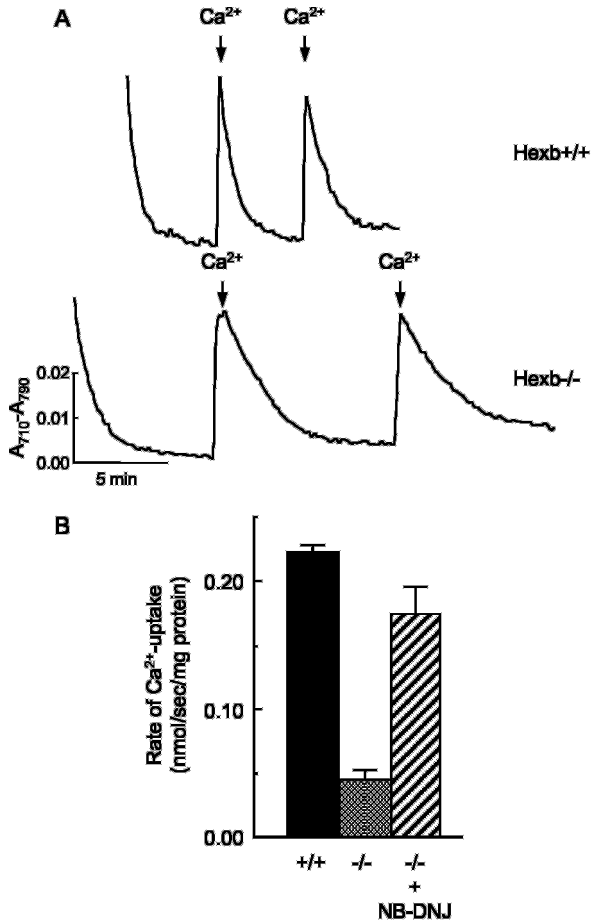

FIG. 2. **Rate of Ca^{2+}-uptake in Hexb microsomes.** *A*, cortical microsomes were loaded by two sequential additions of 25 nmol of Ca^{2+}. Data are representative traces showing absorbance change (A_{710}-A_{790}) of antipyrylazo III *versus* time, with an increase in absorbance demonstrating an increase in free Ca^{2+} in the cuvette and a decrease in absorbance demonstrating a decrease in free Ca^{2+} because of microsomal Ca^{2+}-uptake by SERCA. *B*, the mean rate of Ca^{2+}-uptake ($n = 3$ or 4 ± S.D.) was determined in microsomes obtained from Hexb+/+ and Hexb−/− mice or from Hexb−/− mice that were fed NB-DNJ.

in part, for the neuropathophysiology observed in neuronopathic forms of Gaucher disease, in which glucosylceramide accumulates in lysosomes. To determine whether Ca^{2+}-homeostasis is also affected in Sandhoff disease mice, we examined Ca^{2+}-release and -uptake in Hexb microsomes, by a spectrophotometric assay using the Ca^{2+}-sensitive dye, antipyrylazo III. No differences were detected in the rate of agonist-induced Ca^{2+}-release via the ryanodine or inositol 1,4,5-trisphosphate receptors, the major Ca^{2+}-release channels in the endoplasmic reticulum (ER) (not shown). In contrast, the rate of Ca^{2+}-uptake was reduced by ~5-fold in microsomes from Hexb−/− compared with Hexb+/+ mice (Fig. 2*A*) and, remarkably, was almost completely normal in microsomes from Hexb−/− mice fed with NB-DNJ (Fig. 2*B*). These results suggest a causal relationship between GM2 levels and rates of Ca^{2+}-uptake via SERCA. Although we cannot formally exclude the possibility that NB-DNJ by itself effects SERCA activity *in vivo*, there is no indication from clinical studies (34) or from studies in cell culture (35) that NB-DNJ has any effect on Ca^{2+}-homeostasis, and moreover, no changes are observed in GM2 levels in wild type mice fed NB-DNJ (36). A causal relationship between GM2 levels and SERCA activity was supported by a similar reduction in the rate of Ca^{2+}-uptake in Hexb+/+ microsomes incubated with exogenously added GM2 (Table I). Two other monosialogangliosides, GM3 and GM1, also reduced the rate of Ca^{2+}-uptake but to a smaller extent than GM2 (Table I).

To determine the mechanism by which GM2 affects SERCA activity, we analyzed the initial rate of Ca^{2+}-uptake by a radiometric assay using a rapid filtration technique (21). The V_{max} of SERCA was 3.70 ± 0.12 nmol Ca^{2+}/s/mg of protein in Hexb+/+ brain microsomes and 1.88 ± 0.17 nmol Ca^{2+}/s/mg of protein in Hexb−/− microsomes, the K_{Ca} was 0.29 ± 0.03 and 0.23 ± 0.06 μM for Hexb+/+ and Hexb−/−, respectively, with no change in the Hill coefficient (1.9 *versus* 2.0) (Fig. 3*A*), and there was a small but non-significant reduction in the K_{ATP} (140 ± 40 μM for Hexb+/+ and 80 ± 20 μM for Hexb−/−) (Fig. 3*B*). Thus, GM2 affects the V_{max} of SERCA but not its affinity toward Ca^{2+} or ATP. The reduction in V_{max} was not because of transcriptional regulation of SERCA, because there were no changes in mRNA expression in brain for the SERCA2 isoforms[2] (the predominant isoform in brain (37)) (Fig. 4*A*) and no change in SERCA2 protein levels in microsomes (Fig. 4*B*).

We next examined the functional significance of the reduced

TABLE I
Effect of exogenously-added gangliosides on microsomal Ca^{2+}-uptake

Cortical microsomes were incubated with gangliosides 5 min prior to Ca^{2+}-loading, as in Fig. 2. Results are means ± S.D. for two to four independent analyses.

Ganglioside (10 μM)	Rate of Ca^{2+}-uptake
	nmol/s/mg protein
None	0.22 ± 0.01
GM3	0.17 ± 0.04
GM2	0.07 ± 0.02
GM1	0.13 ± 0.00

[2] Using the primers for SERCA2a, a second product was amplified (Fig. 4*A*). Sequencing revealed a novel SERCA2 isoform with an alternative COOH terminus, designated SERCA2c. This isoform differs from SERCA2a by 83 nucleotides (6879 to 6961; GenBank™ accession no. AJ131870 (19)) inserted between exons 21 and 25. The amino acid sequence of the COOH terminus is LEQPGQS instead of ^{518}LEQPAILE for SERCA2a.

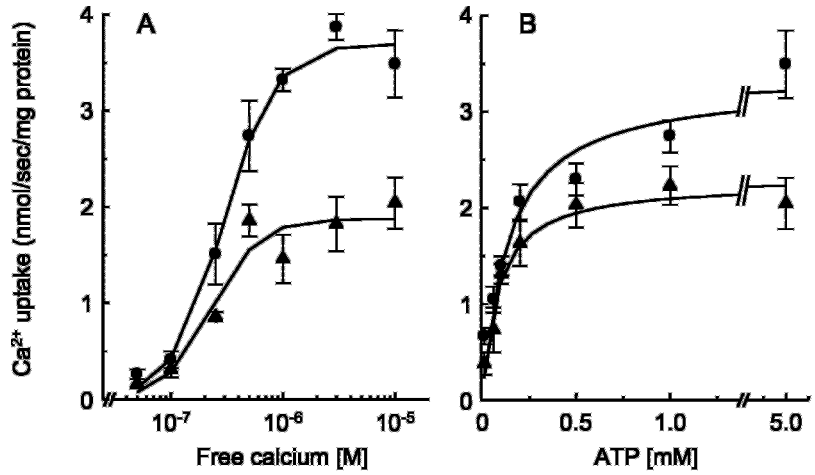

FIG. 3. **Initial rate of Ca^{2+}-uptake in Hexb microsomes.** The initial rate (v_o) of Ca^{2+}-uptake in cortical microsomes from Hexb+/+ (*circles*) or Hexb−/− (*triangles*) mouse brains was measured using $^{45}Ca^{2+}$ varying either free Ca^{2+} (in the presence of 5 mM ATP) (*A*) or ATP (in the presence of 10 μM free Ca^{2+}) (*B*). A best fit was obtained by non-linear regression analysis. Results are means ± S.D. for five to twelve independent measurements using two to three different microsomal preparations.

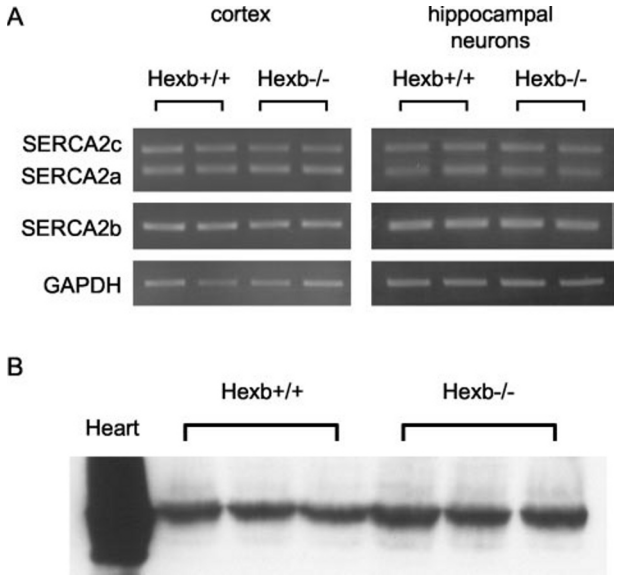

FIG. 4. **RT-PCR and Western blotting of SERCA.** *A*, RT-PCR was performed on RNA extracted from two samples of Hexb+/+ and Hexb−/− cortices or from two cultures of hippocampal neurons; levels of glyceraldehyde-3-phosphate dehydrogenase (*GAPDH*) expression are shown to demonstrate that equal amounts of RNA were used for RT-PCR. One of two independent experiments is shown. *B*, Western blotting using an anti-SERCA antibody was performed on three different microsomal preparations from each Hexb−/− and Hexb+/+ brain (100 μg of protein) or from rat heart (20 μg of protein); note that even though SERCA2 is the predominant SERCA isoform in brain, its levels are much lower than in heart microsomes.

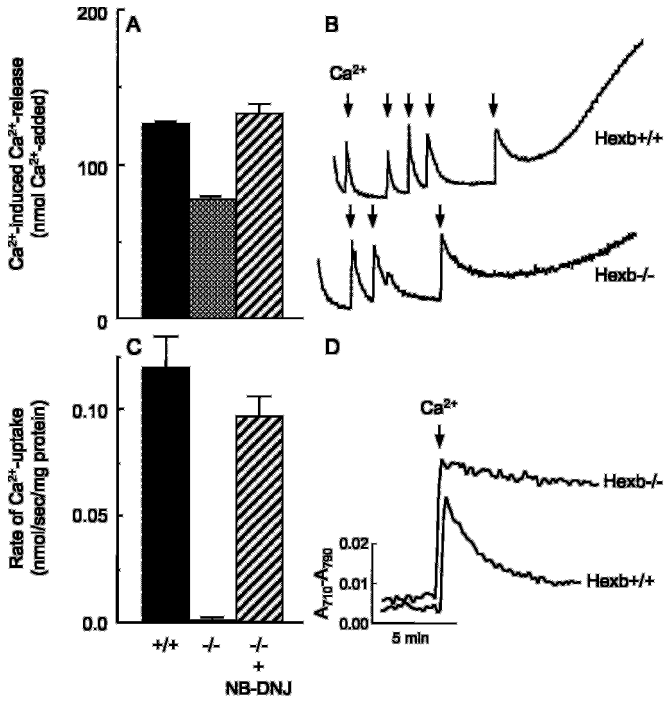

FIG. 5. **CICR and thapsigargin sensitivity.** *A* and *B*, cortical microsomes were loaded by sequential additions of 25 nmol of Ca^{2+} until CICR was induced. *Panel A* gives the average concentration of Ca^{2+} required to induce CICR for microsomes from Hexb+/+ and Hexb−/− microsomes or from microsomes from Hexb−/− mice that were fed NB-DNJ, and *panel B* shows typical traces of absorbance change (A_{710}-A_{790}) of antipyrylazo III *versus* time; in the *upper trace*, CICR is induced after five additions of 25 nmol of Ca^{2+}, whereas in the *bottom trace*, CICR is induced after three additions of 25 nmol of Ca^{2+}. *C* and *D*, cortical microsomes were incubated with 75 μM thapsigargin (not shown), followed by one addition of 25 nmol of Ca^{2+}. *Panel C* gives the rate of Ca^{2+}-uptake after thapsigargin addition, and *panel D* shows typical traces of Ca^{2+}-uptake. Results in *panels A* and *C* are means ± S.D. of three to five independent experiments.

rate of Ca^{2+}-uptake via SERCA. Hexb−/− microsomes were significantly more sensitive to calcium-induced calcium release (CICR) than Hexb+/+ microsomes or microsomes from Hexb−/− mice fed with NB-DNJ (Fig. 5, *A* and *B*), suggesting that elevated cytosolic Ca^{2+} levels in Hexb−/− neurons may induce CICR. In addition, thapsigargin (75 μM), a specific SERCA inhibitor (38), blocked Ca^{2+}-uptake by only 50% in Hexb+/+ microsomes (compare Fig. 2*B* with Fig. 5*C*) but completely blocked SERCA activity in Hexb−/− microsomes (Fig. 5, *C* and *D*), an effect that was again prevented in Hexb−/− microsomes from NB-DNJ-fed mice. To determine whether the enhanced sensitivity to thapsigargin might be of functional significance for neuronal viability, we examined the effect of thapsigargin on neurons cultured from E17 Hexb mice. No changes in mRNA expression of SERCA2 was detected in hippocampal neurons (Fig. 4*A*). Even in neurons from these young mice, a significant reduction in the rate of Ca^{2+}-uptake into the ER of live neurons was observed (Fig. 6*A*), and the rate of Ca^{2+}-uptake into E17 microsomes was also decreased by ~50% (Fig. 6*B*). Note that the specific activity of SERCA in embryonic microsomes was ~50-fold lower than in adult microsomes (compare Fig. 2*B* with Fig. 6*B*), implying that the small but significant amounts of GM2 that accumulate in E17 brain (Fig. 1), and in cultured neurons from E17 embryos (7), is sufficient to account for the reduction in SERCA activity. Intriguingly, neurons cultured from Hexb−/− mice were more sensitive to thapsigargin-induced neuronal cell death than Hexb+/+ neurons, supporting our contention that changes in cytosolic Ca^{2+} levels resulting from inhibition of SERCA activity by GM2 may be

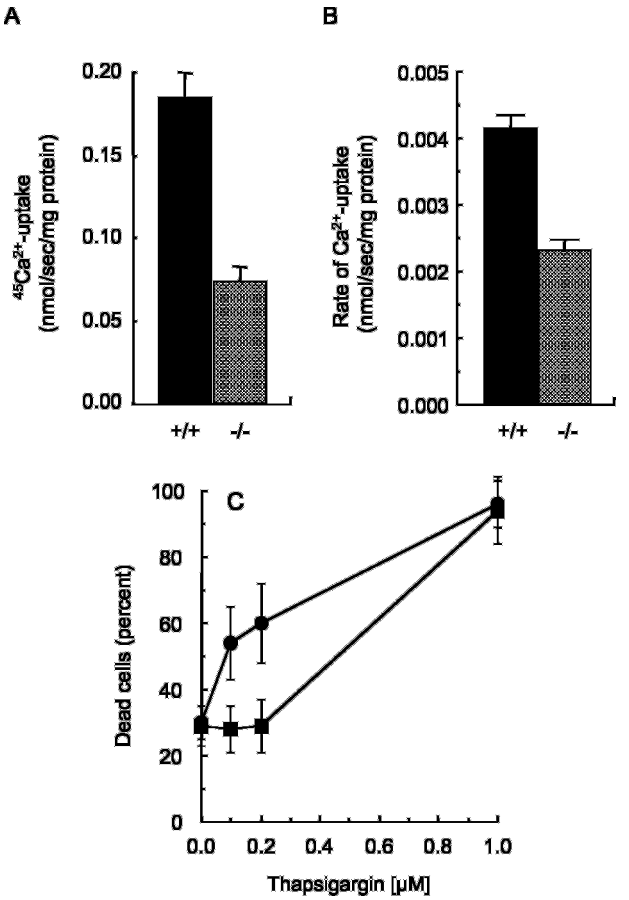

FIG. 6. **Ca^{2+}-Uptake in embryonic hippocampal neurons.** *A*, $^{45}Ca^{2+}$-uptake into 7-day-old neurons cultured from E17 Hexb+/+ and Hexb−/− mice. Results are means ± S.D. from three independent neuronal cultures in which $^{45}Ca^{2+}$-uptake was measured on six individual coverslips. *B*, the mean rate of Ca^{2+}-uptake (n = 3 or 4 ± S.D.) was determined in cortical microsomes from E17 Hexb+/+ and Hexb−/− mice. Results are means ± S.D. for three independent measurements. *C*, 4-day-old neurons cultured from E17 Hexb+/+ (*squares*) or Hexb−/− (*circles*) mice were incubated with thapsigargin for 1 h, and cell death was quantified using the Live/Dead® kit. Results are means ± S.D. for three independent cultures in which four coverslips were analyzed for each thapsigargin concentration.

involved in the molecular mechanism(s) causing neuronal pathophysiology in Sandhoff disease.

DISCUSSION

The major finding of the current study is that ganglioside GM2, upon its accumulation in neuronal tissues from Hexb−/− mice, affects the rate of Ca^{2+}-uptake into brain microsomes and into the ER of live neurons, because of a decrease in the V_{max} of SERCA. As a result, neurons are more sensitive to thapsigargin-induced neuronal cell death, implying that altered Ca^{2+}-uptake may be of physiological relevance for understanding the etiology of Sandhoff disease.

The main functions of SERCA in skeletal and smooth muscle (37) are to prevent prolonged elevation of cytosolic Ca^{2+} and to maintain Ca^{2+} levels within the ER (39). Modification of SERCA activity normally has deleterious effects (40). Less is known about the regulation of SERCA activity in brain, where it occurs at much lower levels than in muscle (41), but a number of studies, mainly using thapsigargin, have shown that SERCA plays a crucial role in neuronal function. For instance, exposure of neurons and neuronal cell lines to thapsigargin results in ER stress (42, 43), decreased neuronal viability (8, 9), inhibition of protein synthesis (44), and injury in developing nerves (45).

Two previous studies have demonstrated that exogenously added gangliosides modulate SERCA activity in rabbit sarcoplasmic reticulum (46, 47), but ours is the first to show a direct physiological link between endogenous ganglioside accumulation and neuronal cell death mediated via SERCA. In the previous studies, GM1 inhibited rabbit sarcoplasmic reticulum SERCA whereas GM3 activated SERCA (47) via a mechanism that was proposed to involve the compactness of the hydrophilic and hydrophobic domains. In our study on mouse brain SERCA, GM1 and GM3 both inhibited SERCA, although exogenously added GM3 had a slight stimulatory effect at higher concentrations (*i.e.* 50 μM) (not shown). Irrespective of the effects of GM3 and GM1, our data unambiguously demonstrate that GM2 has a potent inhibitory effect on SERCA activity and that neurons that accumulate endogenous GM2 are more sensitive to thapsigargin-induced neuronal cell death via a pathway that may be amplified in neurons by their enhanced sensitivity to CICR.

We demonstrated previously (7) that endogenous GM2 accumulation in Hexb−/− neurons results in reduced rates of axonal and dendritic growth but no changes in viability under non-stress conditions. Interestingly, an inverse relationship exists between cytosolic Ca^{2+} levels and rates of axon outgrowth (48), suggesting a mechanistic link among GM2 accumulation, SERCA activity, cytosolic Ca^{2+}, and axonal outgrowth. Clearly, modulation of SERCA activity, either directly or indirectly by GM2, is the critical step in this pathway, and a crucial question concerns whether the intracellular GM2 that accumulates in Hexb−/− brains is accessible to SERCA in neurons, because gangliosides are not normally considered to reside in the ER, as they are synthesized distal to the ER in the Golgi apparatus. Our observation that GM2 is readily detectable in the same microsomes used to analyze SERCA activity lends support to the possibility that SERCA could be directly modulated by GM2. It should be noted that other gangliosides affect intracellular organelles other than those in which they reside or are degraded. For instance, ganglioside GD3 traffics to mitochondria where it affects mitochondrial function (49).

To date, no molecular mechanism has been provided to explain the neuropathophysiology in Sandhoff disease. Microglial activation precedes acute neurodegeneration in Hexb−/− mice, with elevation of various genes related to a macrophage-mediated inflammatory response (50, 51), although the initiating signal for microglial activation is not known. Our data suggest that a downstream response to changes in cytosolic Ca^{2+} levels might initiate a stress response (52), which may subsequently act as an initiating signal for the neuroinflammatory response. Interestingly, the inflammatory response pre-dates symptom onset in Hexb−/− mice (53), and changes in SERCA activity can be detected in mice as young as embryonic day 17, even though no symptoms of Sandhoff disease are observed until 2–3 months of age. Moreover, the ability of NB-DNJ to prevent the reduction of SERCA activity, because of a decrease in storage levels of GM2, together with the delayed symptom onset of these mice (12), implies a direct correlation between the initiation of neuronal cell dysfunction and/or death and modulation of SERCA activity by GM2.

Acknowledgments—We thank Niv Tutka from the Experimental Animal Center (Weizmann Institute of Science) for maintaining the Hexb mouse colony, Revital Benvenisti and Omer Peretz for genotyping the Hexb colony, and Steve Karlish (Weizmann Institute of Science) for helpful comments.

REFERENCES

1. Gravel, R. A., Kaback, M. M., Proia, R., Sandhoff, K., Suzuki, K., and Suzuki, K. (2001) in *The Metabolic and Molecular Bases of Inherited Disease* (Scriver, C. R., Sly, W. S., Childs, B., Beaudet, A. L., Valle, D., Kinzler, K. W., and Vogelstein, B., eds) pp. 3827–3876, McGraw-Hill Inc., New York

2. Kolter, T., and Sandhoff, K. (1998) *J. Inherit. Metab. Dis.* **21,** 548–563
3. Mahuran, D. J. (1999) *Biochim. Biophys. Acta* **1455,** 105–138
4. Jeyakumar, M., Butters, T. D., Dwek, R. A., and Platt, F. M. (2002) *Neuropathol. Appl. Neurobiol.* **28,** 343–357
5. Sango, K., Yamanaka, S., Hoffmann, A., Okuda, Y., Grinberg, A., Westphal, H., McDonald, M. P., Crawley, J. N., Sandhoff, K., Suzuki, K., and Proia, R. L. (1995) *Nat. Genet.* **11,** 170–176
6. Sango, K., McDonald, M. P., Crawley, J. N., Mack, M. L., Tifft, C. J., Skop, E., Starr, C. M., Hoffmann, A., Sandhoff, K., Suzuki, K., and Proia, R. L. (1996) *Nat. Genet.* **14,** 348–352
7. Pelled, D., Riebeling, C., van Echten-Deckert, G., Sandhoff, K., and Futerman, A. H. (2003) *Neuropathol. Appl. Neurobiol.*, in press
8. Nguyen, H. N., Wang, C., and Perry, D. C. (2002) *Brain Res.* **924,** 159–166
9. Wei, H., Wei, W., Bredesen, D. E., and Perry, D. C. (1998) *J. Neurochem.* **70,** 2305–2314
10. Platt, F. M., Neises, G. R., Dwek, R. A., and Butters, T. D. (1994) *J. Biol. Chem.* **269,** 8362–8365
11. Platt, F. M., Neises, G. R., Reinkensmeier, G., Townsend, M. J., Perry, V. H., Proia, R. L., Winchester, B., Dwek, R. A., and Butters, T. D. (1997) *Science* **276,** 428–431
12. Jeyakumar, M., Butters, T. D., Cortina-Borja, M., Hunnam, V., Proia, R. L., Perry, V. H., Dwek, R. A., and Platt, F. M. (1999) *Proc. Natl. Acad. Sci. (U. S. A.)* **96,** 6388–6393
13. Sango, K., Yamanaka, S., Ajiki, K., Takashikim, A., and Watabe, K. (2002) *Neuropathol. Appl. Neurobiol.* **28,** 23–34
14. Hirschberg, K., Zisling, R., van Echten-Deckert, G., and Futerman, A. H. (1996) *J. Biol. Chem.* **271,** 14876–14882
15. van Echten-Deckert, G., Giannis, A., Schwarz, A., Futerman, A. H., and Sandhoff, K. (1998) *J. Biol. Chem.* **273,** 1184–1191
16. Betto, R., Teresi, A., Turcato, F., Salviati, G., Sabbadini, R. A., Krown, K., Glembotski, C. C., Kindman, L. A., Dettbarn, C., Pereon, Y., Yasui, K., and Palade, P. T. (1997) *Biochem. J.* **322,** 327–333
17. Bradford, M. (1976) *Anal. Biochem.* **72,** 248–254
18. Palade, P. (1987) *J. Biol. Chem.* **262,** 6149–6154
19. Ver Heyen, M., Reed, T. D., Blough, R. I., Baker, D. L., Zilberman, A., Loukianov, E., Van Baelen, K., Raeymaekers, L., Periasamy, M., and Wuytack, F. (2000) *Mamm. Genome* **11,** 159–163
20. Dettbarn, C., Betto, R., Salviati, G., Sabbadini, R., and Palade, P. (1995) *Brain Res.* **669,** 79–85
21. Ji, Y., Loukianov, E., and Periasamy, M. (1999) *Anal. Biochem.* **269,** 236–244
22. Imagawa, T., Smith, J. S., Coronado, R., and Campbell, K. P. (1987) *J. Biol. Chem.* **262,** 16636–16643
23. Fabiato, A., and Fabiato, F. (1979) *J. Physiol. (Paris)* **75,** 463–505
24. Wells, K. M., and Abercrombie, R. F. (1998) *J. Biol. Chem.* **273,** 5020–5025
25. Cornea, R. L., Autry, J. M., Chen, Z., and Jones, L. R. (2000) *J. Biol. Chem.* **275,** 41487–41494
26. Bodennec, J., Pelled, D., Riebeling, C., Trajkovic, S., and Futerman, A. H. (2002) *FASEB J.* **16,** 1814–1816
27. Riebeling, C., Forsea, A. M., Raisova, M., Orfanos, C. E., and Geilen, C. C. (2002) *Br. J. Cancer.* **87,** 366–371
28. Brewer, G. J., Torricelli, J. R., Evege, E. K., and Price, P. J. (1993) *J. Neurosci. Res.* **35,** 567–576
29. Korkotian, E., Schwarz, A., Pelled, D., Schwarzmann, G., Segal, M., and Futerman, A. H. (1999) *J. Biol. Chem.* **274,** 21673–21678
30. Sofer, A., Schwarzmann, G., and Futerman, A. H. (1996) *J. Cell Sci.* **109,** 2111–2119
31. Deber, C. M., and Hsu, L. C. (1986) *Biochem. Biophys. Res. Commun.* **134,** 731–735
32. Fields, A., Gafni, Y., Oron, Y., and Sarne, Y. (1995) *Brain Res.* **687,** 94–102
33. Lloyd-Evans, E., Pelled, D., Riebeling, C., Bodennec, J., de-Morgan, A., Waller, H., Schiffmann, R., and Futerman, A. H. (2003) *J. Biol. Chem.*, **278,** 23594–23599
34. Cox, T., Lachmann, R., Hollak, C., Aerts, J., van Weely, S., Hrebicek, M., Platt, F., Butters, T., Dwek, R., Moyses, C., Gow, I., Elstein, D., and Zimran, A. (2000) *Lancet* **355,** 1481–1485
35. Bieberich, E., MacKinnon, S., Silva, J., and Yu, R. K. (2001) *J. Biol. Chem.* **276,** 44396–44404
36. Platt, F. M., Reinkensmeier, G., Dwek, R. A., and Butters, T. D. (1997) *J. Biol. Chem.* **272,** 19365–19372
37. Misquitta, C. M., Mack, D. P., and Grover, A. K. (1999) *Cell Calcium* **25,** 277–290
38. Treiman, M., Caspersen, C., and Christensen, S. B. (1998) *Trends Pharmacol. Sci.* **19,** 131–135
39. MacLennan, D. H. (2000) *Eur. J. Biochem.* **267,** 5291–5297
40. Frank, K. F., Bolck, B., Brixius, K., Kranias, E. G., and Schwinger, R. H. (2002) *Basic Res. Cardiol.* **97,** 172–178
41. East, J. M. (2000) *Mol. Membr. Biol.* **17,** 189–200
42. Paschen, W., Mengesdorf, T., Althausen, S., and Hotop, S. (2001) *J. Neurochem.* **76,** 1916–1924
43. Mengesdorf, T., Althausen, S., Oberndorfer, I., and Paschen, W. (2001) *Biochem. J.* **356,** 805–812
44. Doutheil, J., Treiman, M., Oschlies, U., and Paschen, W. (1999) *Cell Calcium* **25,** 419–428
45. Turner, C. P., Pulciani, D., and Rivkees, S. A. (2002) *Exp. Neurol.* **178,** 21–32
46. Wang, L. H., Tu, Y. P., Yang, X. Y., Tsui, Z. C., and Yang, F. Y. (1996) *FEBS Lett.* **388,** 128–130
47. Wang, Y., Tsui, Z., and Yang, F. (1999) *FEBS Lett.* **457,** 144–148
48. Tang, F., Dent, E. W., and Kalil, K. (2003) *J. Neurosci.* **23,** 927–936
49. Garcia-Ruiz, C., Colell, A., Morales, A., Calvo, M., Enrich, C., and Fernandez-Checa, J. C. (2002) *J. Biol. Chem.* **277,** 36443–36448
50. Wada, R., Tifft, C. J., and Proia, R. L. (2000) *Proc. Natl. Acad. Sci. (U. S. A.)* **97,** 10954–10959
51. Myerowitz, R., Lawson, D., Mizukami, H., Mi, Y., Tifft, C. J., and Proia, R. L. (2002) *Hum. Mol. Genet.* **11,** 1343–1350
52. Wyss-Coray, T., and Mucke, L. (2002) *Neuron* **35,** 419–432
53. Jeyakumar, M., Thomas, R., Elliot-Smith, E., Smith, D. A., van der Spoel, A. C., d'Azzo, A., Perry, V. H., Butters, T. D., Dwek, R. A., and Platt, F. M. (2003) *Brain* **126,** 974–987